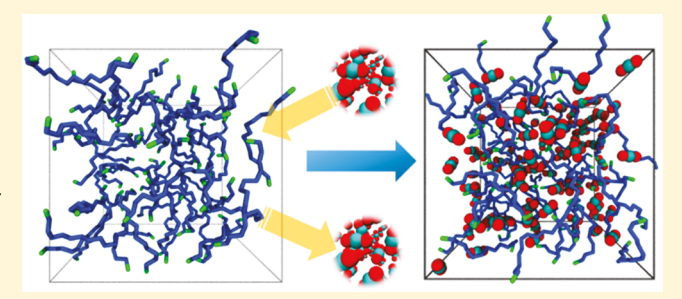


Molecular Simulation Study on the Volume Swelling and the Viscosity Reduction of n-Alkane/CO₂ Systems

Chuncheng Li,† Hui Pu,*,† and Julia Xiaojun Zhao*,‡ D

ABSTRACT: Carbon dioxide (CO₂) injection is a successful enhanced oil recovery (EOR) technology that is being widely applied in North American oil fields. Studies have suggested CO₂-based EOR is technically possible in the Middle Bakken Formation of the Williston Basin in North Dakota. The swelling of a crude oil/CO2 mixture plays a crucial role in the CO₂ flooding process. Therefore, a better understanding of the effect of CO2 on crude oil swelling and viscosity reduction is critical for a successful CO2 EOR project in unconventional reservoirs such as the Bakken Formation. In this work, a series of n-alkane/CO2 systems were studied by performing



configurational-bias Monte Carlo (CBMC) simulations and molecular dynamics (MD) simulations. The effects of carbon chain length, pressure, and temperature on the CO₂ solubility and the swelling factor were investigated. The solubility of CO₂ and the swelling factor of the CO₂-saturated n-alkane are positively correlated to the pressure, while negatively correlated to the carbon chain length and temperature. With more CO₂ dissolved, the interaction energy between n-alkane molecules becomes less negative, which indicates the swelling of the n-alkane/CO2 system. n-Alkanes with a longer carbon chain have a more negative intermolecular interaction energy and thus have a smaller swelling factor after saturation with CO₂. With the increase of the CO₂ mole fraction, the viscosity of the n-alkane/CO₂ system is reduced. n-Alkanes with longer carbon chains have a larger viscosity reduction with increasing amounts of dissolved CO2. This study provides a reliable assessment of the volume swelling and viscosity reduction of n-alkane/CO₂ systems and can further assist the CO₂ EOR application in the Bakken Formation.

1. INTRODUCTION

Resulting in incremental oil recovery as well as reducing carbon dioxide (CO₂) emission, CO₂ injection has become one of the most common enhanced oil recovery (EOR) techniques in North America. Many CO2 injection projects have been successfully carried out in Texas, New Mexico, and Colorado.²⁻⁴ In recent years, the Middle Bakken formation of the Williston Basin in North Dakota has become the interest of CO2 EOR applications. The Middle Bakken formation is a typical tight formation, which holds a huge CO₂ storage capacity and the potential of significantly increasing oil production by injection of CO₂.⁵ The predicted recovery factor of primary oil recovery is less than 10%, 6,7 while using the CO₂ injection technique a 2.5-9.4% incremental oil recovery factor can be obtained.8

Swelling of crude oil by dissolved CO2 and reduction of crude oil viscosity are two main physical mechanisms of the CO₂ EOR method. 9,10 When CO₂ is injected into a reservoir and contacts the crude oil, the dissolution of CO₂ occurs, thereby causing swelling and density reduction. The swollen oil droplets will increase the oil saturation and the reservoir pressure. Some trapped oil will be forced out of the pore spaces and move toward the fractures or the production well. Thus, additional oil can be recovered from reservoirs. The system

expansion process can reduce crude oil viscosity significantly and, therefore, increase the mobility of crude oil. Some experiments $^{11-15}$ focusing on the $\rm CO_2$ dissolution and

swelling effect have been carried out, and various models and correlations 16-19 have been built to predict the CO₂ solubility, crude oil/CO2 mixture viscosity, oil swelling factor, etc. However, experimental studies are often time-consuming and costly and cannot cover all the conditions, especially for CO₂crude oil interactions in micro- and/or nanopore spaces in tight formations. Although models and correlations can predict many parameters easily, they cannot explain different phenomena scientifically and thoroughly.

Over the past few years, molecular simulation methods including the Monte Carlo (MC) method and the molecular dynamics (MD) method have been widely used to study the gas solubility and diffusion coefficient in liquids and the viscosity of gas/liquid mixtures. ^{20–25} Zhang et al. ²³ provided a reasonable method to study the CO2 solubility in octane and the swelling of the octane/CO₂ system with a MC simulation.

Received: March 6, 2019 Revised: April 17, 2019 Accepted: May 2, 2019 Published: May 2, 2019

Department of Petroleum Engineering, University of North Dakota, Grand Forks, North Dakota 58202, United States

^{*}Department of Chemistry, University of North Dakota, Grand Forks, North Dakota 58202, United States

Liu et al. 24 used MD simulations to investigate the effects of temperature, pressure, and alkane structures on the swelling of alkane/ CO_2 systems. They inferred that the dispersion interaction is the main reason for the swelling of the alkane/ CO_2 system. Moultos et al. 25 studied the CO_2 diffusivity in various hydrocarbons and reproduced the liquid viscosities with three different force fields.

While the minimum miscibility pressure (MMP) between Bakken crude oil and CO2 as well as CO2 flow in tight Bakken rocks were studied, 5,26,27 more work needs to be done on the solubility of CO2 in Bakken crude oil, the swelling factors of the crude oil/CO2 system, and the crude oil viscosity reduction. In this study, five main *n*-alkanes (octane, decane, dodecane, tetradecane, and hexadecane) in Middle Bakken crude oil²⁸ were selected, and a series of configurational-bias Monte Carlo (CBMC)^{29,30} simulations were performed to study the impacts of pressure, temperature, and carbon chain length on the solubility of CO2 in different n-alkanes and the swelling of n-alkane/CO2 systems. MD simulations were carried out to study the viscosity reduction of n-alkanes due to the dissolution of CO₂. The main temperature employed in our simulations is 383 K, which is consistent with the reported experimental study. 5,26,27

This paper is arranged in the following manner. In Section 2 the force fields employed in the study and the simulation details are discussed. In Section 3 the simulation results and discussions are presented. Finally, in Section 4 the assessment of our study and the conclusions are offered.

2. FORCE FIELDS AND SIMULATION DETAILS

2.1. Force Fields. The non-bonded interactions for the force fields employed in this work were described by the pairwise additive Lennard–Jones (LJ) 12–6 potentials and the Coulombic interactions given by

$$U(r_{ij}) = 4\varepsilon_{ij} \left[\left(\frac{\sigma_{ij}}{r_{ij}} \right)^{12} - \left(\frac{\sigma_{ij}}{r_{ij}} \right)^{6} \right] + \frac{q_{i}q_{j}}{4\pi r_{ij}}$$

$$\tag{1}$$

where ε_{ij} donates the depth of the potential well, σ_{ij} represents the distance at which the interaction energy of two particles is minimal, r_{ij} is the distance between particles i and j, and q_i and q_i are the partial charges for particles i and j, respectively.

In the CBMC simulations, the nonpolar, flexible chain *n*-alkane molecules were described by the transferable potentials for the phase equilibria united-atom (TraPPE-UA) model, ^{31,32} in which methyl (CH₃) and methylene (CH₂) groups were treated as pseudoatoms. The Lorentz–Berthelot combining rules were used to determine the cross-parameters for unlikepair interactions. While, in the MD simulations, the L-OPLS-AA force field ³³ was selected to describe the *n*-alkanes, as this force field is more accurate in reproducing the viscosity of long-chain alkanes.³⁴ The unlike interactions were evaluated using the geometric mean combining rule. The CO₂ molecules were described by the TraPPE model³⁵ with two rigid bonds and a rigid bond angle.

The non-bonded and bonded parameters for each of the force fields used in this work are listed in Tables 1–4, respectively.

2.2. Simulation Details. The CBMC simulations were performed with a fixed number of 100 *n*-alkane molecules in a cubic unit cell for both pure and CO₂-saturated *n*-alkane systems. The Monte Carlo moves of *n*-alkane molecules were

Table 1. Parameters for Non-Bonded Interactions Used in CBMC Simulations

atom/group ^a	q_i (e)	σ_{ii} (Å)	$arepsilon_{ii}$ (kcal mol $^{-1}$)
CH ₃	0	3.75	0.195
CH_2	0	3.95	0.0914
С	0.70	2.80	0.0537
O	-0.35	3.05	0.157

^aNote: C represents the C in CO₂, and O represents the O in CO₂.

translation, rotation, and reinsertion. The relative frequency of the three moves was 1:1:1. For CO₂-saturated n-alkane systems, with the insertion and deletion of CO₂ molecules, the systems reached equilibrium at specified temperatures and pressures. The Monte Carlo moves of CO₂ molecules were translation, rotation, reinsertion, and swap. The relative frequency of the four moves was 1:1:1:1. The grand canonical (μVT) ensemble^{23,36} was employed for the simulations of CO₂-saturated *n*-alkane systems. In this ensemble, the temperature, T, the volume, V, and the chemical potential, μ , were fixed. The system volume was allowed to change when the *n*-alkane was absorbing/desorbing CO₂. The volume change probability was set as 0.05. The total energy, density, and number of CO₂ molecules were monitored to check the equilibration conditions. A truncated and shifted potential with a cutoff radius of 12 Å was used. The number of initialization cycles and production cycles was 10000 and 50000, respectively. The simulations were performed for a pressure range of 2-10 MPa and a temperature range of 323-383 K. Finally, the average values of the properties of interest were calculated and analyzed.

Equilibrium molecular dynamics (EMD) simulations were used in conjunction with the Green–Kubo relation^{37,38} (eq 2) to compute the shear viscosity of the n-alkane/CO₂ systems.

$$\eta(t) = \frac{V}{k_{\rm B}T} \int_0^\infty \langle P_{\alpha\beta}(t_0) P_{\alpha\beta}(t_0 + t) \rangle \, \mathrm{d}t \tag{2}$$

Here, V is the volume of the simulation box, $k_{\rm B}$ is the Boltzmann constant, T is the temperature, $P_{\alpha\beta}$ denotes the off-diagonal components of the pressure tensor, and the angle brackets indicate the ensemble average.

One hundred twenty-five n-alkane molecules and CO₂ molecules with different mole fractions were randomly placed in a cubic box. The box was then equilibrated in the isothermal-isobaric (NPT) ensemble for 3 ns. The average volume of the simulation box during the final 1 ns was calculated and employed in the following 5 ns canonical ensemble (NVT) simulation. The long-range electrostatic interactions were calculated using the particle-particle particle-mesh (PPPM) method³⁹ with an accuracy of 10⁻⁵ and a cutoff radius of 14 Å. The Nosé-Hoover thermostat 40,41 and Parrinello-Rahman barostat 42 were applied to control the temperature and pressure, respectively. Fast-moving bonds involving hydrogen atoms were constrained with the SHAKE algorithm, 43 and the time step was set to 2 fs. The sample interval, correlation length, and dump interval were set to 10, 400, and 4000 timesteps, respectively. The viscosity was finally obtained from the last 2 ns NVT production run based on three independent trajectories.

All CBMC simulations were carried out with the open source package RASPA $2.0.^{44}$ The MD simulations were performed using the LAMMPS package. The configuration

Table 2. Parameters for Bonded Interactions Used in CBMC Simulations^a

stretch		r_0 (Å)	k _b (kcal m	$k_{\rm b}~({\rm kcal~mol^{-1}~\AA^{-2}})$	
CH_x - CH_y		1.54	191	191.77	
C-O		1.16	-		
bend $CH_x-CH_2-CH_y$ $C-O-C$		θ_0 (deg)	$k_{ heta}$ (kcal mol $^{-1}$ rad $^{-2}$) 124.20		
		114.0			
C-O-C		180.0	-	_	
torsion	C_1 (kcal mol ⁻¹)	C_2 (kcal mol ⁻¹)	C_3 (kcal mol ⁻¹)	C_4 (kcal mol ⁻¹)	
CH_x - CH_2 - CH_2 - CH_y	0	0.666	-0.136	1.573	
^a Note: $x = 2$ or 3; $y = 2$ or 3.					

Table 3. Parameters for Non-Bonded Interactions Used in MD Simulations

atom ^a	q_i (e)	$\sigma_{ii} \ (ext{Å})$	ε_{ii} (kcal mol ⁻¹)
CT_CH_3	-0.222	3.50	0.066
CT_CH_2	-0.148	3.50	0.066
HC_CH_3	0.074	2.50	0.03
HC_CH_2	0.074	2.50	0.0263
С	0.70	2.80	0.0537
O	-0.35	3.05	0.157

"Note: CT represents C in in the alkane; HC represents H in the alkane. C represents C in CO_2 ; O represents O in CO_2 .

snapshots were rendered by VMD software. 46 The snapshots of the systems simulated in this work are shown in Figure 1.

3. RESULTS AND DISCUSSION

3.1. CO₂ Solubility in *n*-Alkanes. The definition of CO₂ solubility in an n-alkane is the maximum quantity of CO₂ that can dissolve in a certain quantity of the *n*-alkane at a specified temperature or pressure. The swap move imposes a chemical equilibrium between the system and an imaginary reservoir for CO₂ molecules. Below the concentration of solubility, the chemical potential of CO₂ in the solution is lower than that of the pure CO₂, so CO₂ molecules will transfer from the reservoir to the system until the saturation is reached. The solubility of CO₂ in each *n*-alkane as a function of pressure and temperature is presented in Figures 2 and 3, respectively. For each n-alkane, the solubility of CO₂ increases with the increasing pressure and decreases with the increasing temperature. As shown in Figure 2, at 383 K, the solubility of CO₂ in n-alkanes with different carbon chain lengths varies slightly at a low pressure (2 MPa), while CO₂ is more soluble in *n*-alkanes with shorter carbon chain length at a high pressure (10 MPa).

At the temperature of 383 K, the standard deviations of CO_2 solubility of five n-alkanes at five different pressures (2, 4, 6, 8, and 10 MPa) are 0.93, 2.59, 4.46, 7.93, and 13.14, respectively. At 383 K and 10 MPa, the solubility of CO_2 in n-octane is 2.09 times the solubility of CO_2 in n-hexadecane. Similarly, under the same pressure condition (6 MPa), the difference in solubility of CO_2 in n-alkanes between short-chain n-alkanes and long-chain n-alkanes at a low temperature (323 K) is much larger than that at a high temperature (383 K), as shown in Figure 3. At the pressure of 6 MPa, the standard deviations of CO_2 solubility of five n-alkanes at three different temperatures (323, 353, and 383 K) are 15.66, 7.21, and 4.46, respectively. At 323 K and 6 MPa, the solubility of CO_2 in n-octane is 1.92 times the solubility of CO_2 in n-hexadecane.

3.2. Density of Pure *n***-Alkanes and CO**₂**-Saturated** *n***-Alkanes.** The simulated density values of the pure *n*-alkanes are consistent with the experimental data provided in the National Institute of Standards and Technology (NIST) database. As shown in Figures 4 and 5, the density of pure *n*-alkanes increases slightly with the increasing pressure and the decreasing temperature, while the density of CO₂-saturated *n*-alkanes decreases dramatically with the increasing pressure and the decreasing temperature. The reason for this phenomenon can be explained by the impacts of pressure and temperature on the solubility of CO₂ in *n*-alkane. With the increasing pressure and the decreasing temperature, more CO₂ can dissolve in *n*-alkane, resulting in the expansion of the *n*-alkane, and thus the density of the *n*-alkane decreases.

3.3. Swelling Factor of n-Alkane/CO₂ Systems. The swelling factor, an important indicator for quantifying the oil swelling when CO_2 dissolves into oil, is defined as the volume of the saturated CO_2 -oil mixture divided by the volume of the oil alone. The swelling factor of the n-alkanes/ CO_2 system as a function of pressure and temperature is presented in Figures

Table 4. Parameters for Bonded Interactions Used in MD Simulations

stretch		r_0 (Å) $k_{ m b}$ (kcal mol $^{-1}$ Å $^{-2}$)		$nol^{-1} Å^{-2}$	
CT_CT		1.529	26	268.0	
CT_HC		1.090	34	340.0	
C-O		1.16	-	_	
bend		θ_0 (deg)	$k_{ heta}$ (kcal m	nol ⁻¹ rad ⁻²)	
CT_CT_CT		112.7	58	3.35	
CT_CT_HC		110.7	37.5		
HC_CT_HC		107.8	33.0		
C-O-C		180.0	_	•	
torsion	C_1 (kcal mol ⁻¹)	C_2 (kcal mol ⁻¹)	C_3 (kcal mol ⁻¹)	C_4 (kcal mol ⁻¹)	
CT_CT_CT_CT	0.645	-0.214	0.178	0.000	
CT_CT_CT_HC	0.000	0.000	0.300	0.000	
HC_CT_CT_HC	0.000	0.000	0.300	0.000	

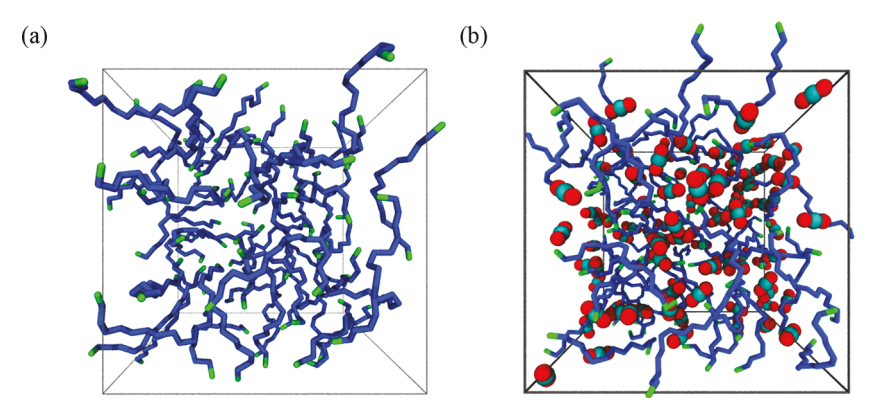


Figure 1. Simulation unit cells of (a) pure and (b) CO₂-saturated hexadecane (green and blue tubes represent the CH₃ group and CH₂ group, respectively; red and cyan spheres represent O atoms and C atoms, respectively).

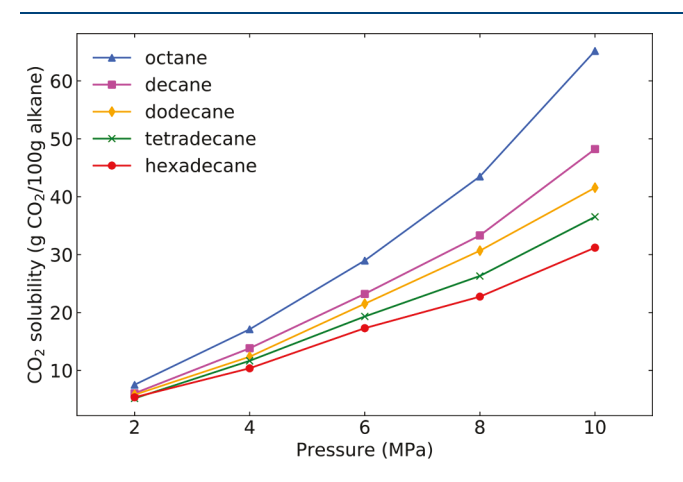


Figure 2. CO_2 solubility in *n*-alkanes as a function of pressure at 383 K.

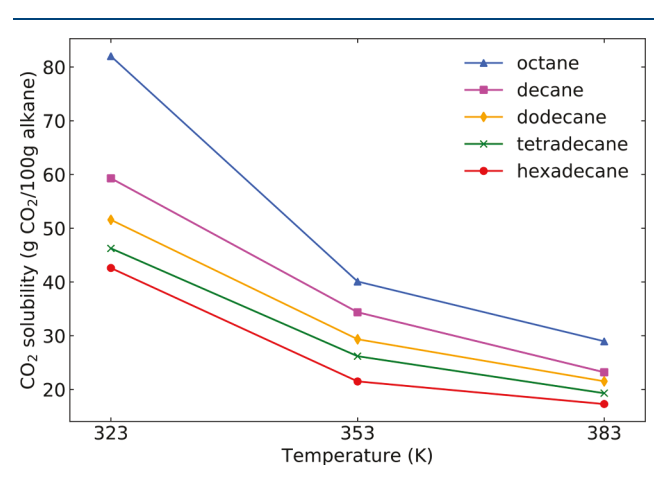


Figure 3. CO_2 solubility in n-alkanes as a function of temperature at 6 MPa.

6 and 7. The swelling factor of the *n*-alkanes/CO₂ system increases with increasing pressure and decreasing temperature, which is consistent with the CO₂ solubility in *n*-alkanes. *n*-Alkanes with a shorter chain length have a higher swelling factor when saturated with CO₂, which indicates that light oil has a higher swelling factor than heavy oil. The simulation results agree well with the experimental ones in ref 16. The swelling factor is a function of the amount of dissolved CO₂ as well as the size of the oil molecules.

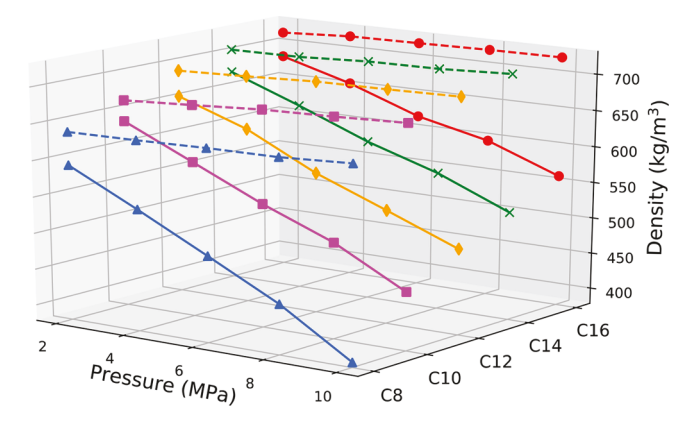


Figure 4. Density of pure (dashed lines) and CO₂-saturated (solid lines) *n*-alkanes as a function of pressure at 383 K.

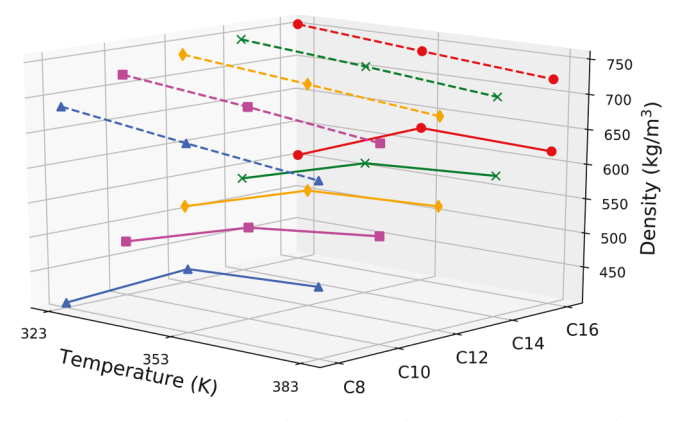


Figure 5. Density of pure (dashed lines) and CO_2 -saturated (solid lines) n-alkanes as a function of temperature at 6 MPa.

3.4. Interaction Energy. As the *n*-alkane molecule and CO₂ molecule are both nonpolar, the intermolecular forces both belong to the London dispersion force, and we would expect that they are soluble in each other. The interactions of these molecules arise solely from the dispersion energy, which will be referred to as the "interaction energy" in this paper. The interaction energies of pure *n*-alkanes at specified pressures and temperatures are calculated, as shown in Figure 8. The *n*-alkanes with shorter chains have a less negative intermolecular interaction energy, which means it is easier for molecules to separate from each other, so a higher swelling factor can be observed when octane is saturated with CO₂.

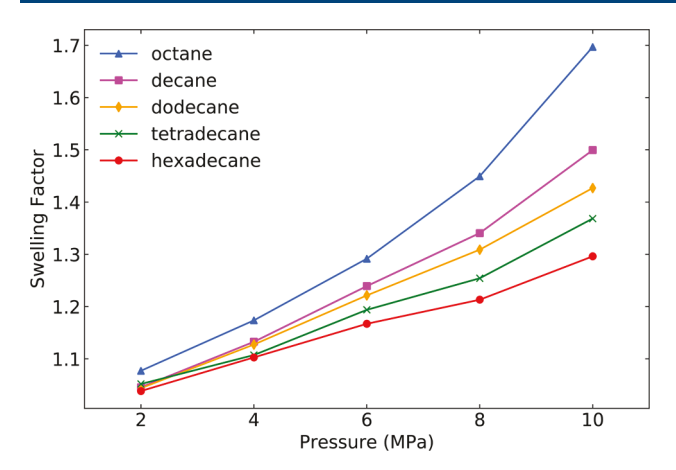


Figure 6. Swelling factor of n-alkane/ CO_2 system as a function of pressure at 383 K.

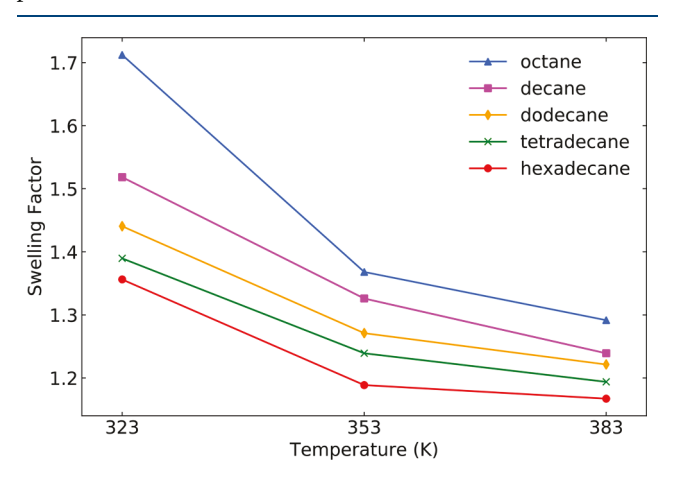


Figure 7. Swelling factor of n-alkane/ CO_2 system as a function of temperature at 6 MPa.

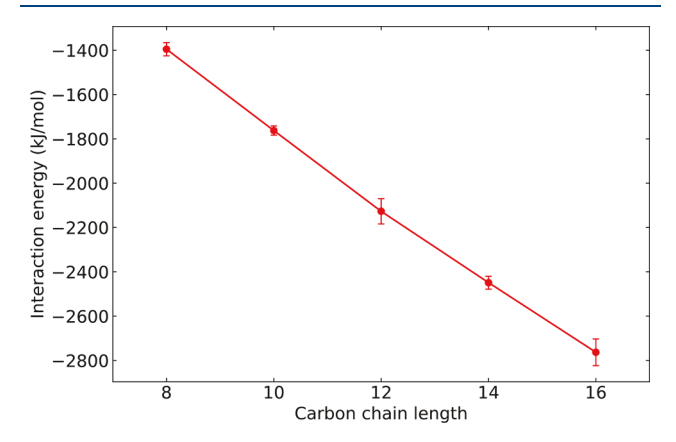


Figure 8. Interaction energy of pure n-alkane molecules at 383 K and 10 MPa.

The interaction energy of n-alkane-n-alkane, CO_2-CO_2 , and n-alkane $-CO_2$ in the n-alkane/ CO_2 system are also analyzed. Taking hexadecane (Figure 9) as an example, the interaction energy between hexadecane and CO_2 molecules becomes more negative with the increasing pressure, while the interaction energy between hexadecane molecules becomes less negative. This is because more CO_2 molecules dissolve in the hexadecane and occupy the intermolecular space of hexadecane molecules.

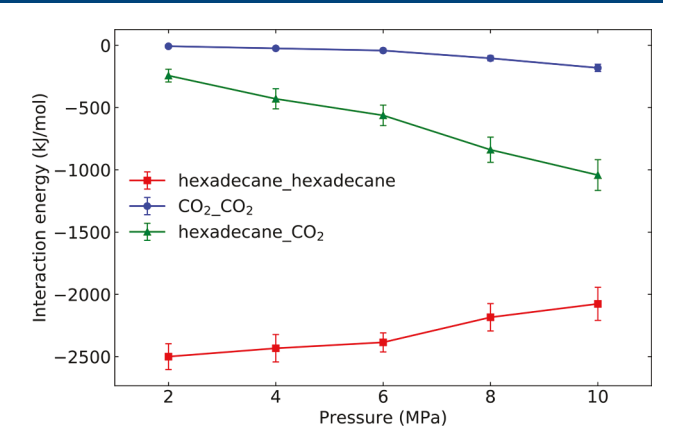


Figure 9. Interaction energy as a function of pressure in the hexadecane/ CO_2 system at 383 K.

The less negative n-alkane—n-alkane interaction energy with the increasing pressure indicates that the diffusion capacity of oil molecules increases when more CO_2 molecules are dissolved. Both the oil— CO_2 interaction and the CO_2 — CO_2 interaction are responsible for the oil swelling. In contrast with the oil— CO_2 interaction energy, the CO_2 — CO_2 interaction energy contributes a tiny amount to the total interaction energy. As a consequence, the oil swelling is predominantly due to the oil— CO_2 interaction.

3.5. Viscosity Reduction of *n***-Alkane/CO**₂ **System.** The viscosities of pure *n*-alkanes and CO₂ at 383 K and 35 MPa are computed and compared with the experimental data in the NIST database. All of the simulation results are in good agreement with the NIST data, yielding a viscosity value within 4% of the experimental one (except 9.5% for dodecane), as shown in Figure 10.

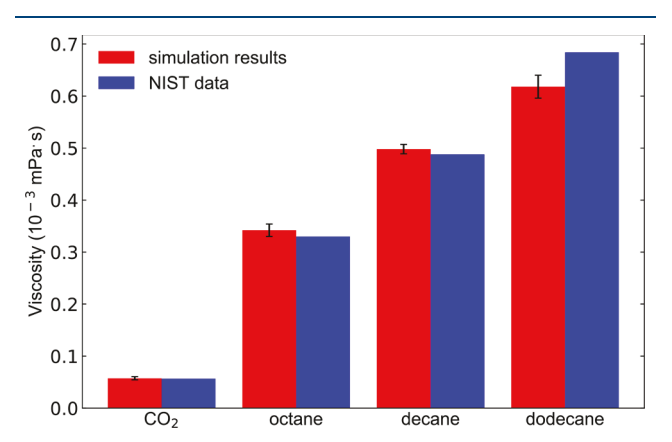


Figure 10. Interaction energy as a function of pressure in the hexadecane/CO₂ system at 383 K.

With the increase of the CO_2 mole fraction, the viscosity of the n-alkane/ CO_2 system is reduced (Figure 11). The viscosity and the CO_2 mole fraction are approximately in a linear relationship. The slopes of these viscosity trend lines (dotted lines in Figure 11) show that the n-alkanes with longer carbon chains have a larger viscosity reduction with increasing CO_2 mole fraction. The average viscosity reduction rate is about 45% when the CO_2 mole fraction is 60%.

The viscosity of crude oil is reduced dramatically when dissolving CO_2 in oil, but it is still much higher than the CO_2 viscosity. When CO_2 is injected into a reservoir, it possibly will

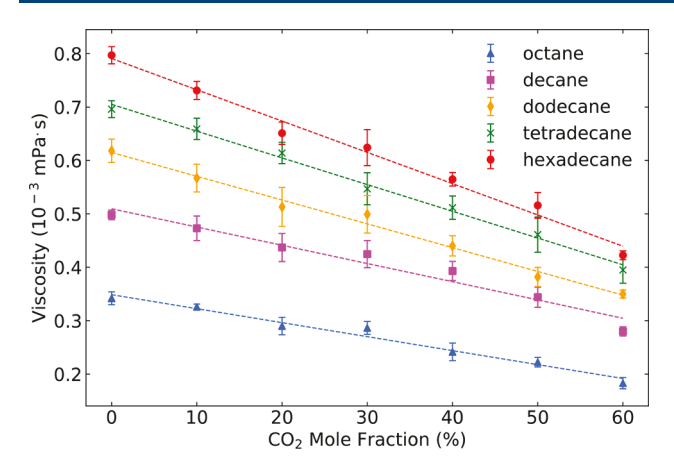


Figure 11. Viscosity of n-alkane/CO $_2$ system as a function of CO $_2$ mole fraction at 383 K and 35 MPa.

cause early breakthrough of CO_2 because of its low viscosity and high mobility, which reduces the sweep efficiency. CO_2 foam or CO_2 emulsion can viscosify the CO_2 and further enhance the oil recovery. In future studies, we will focus on the interactions between the crude oil and CO_2 confined in nanopores and the methods to improve CO_2 sweep efficiency.

4. CONCLUSIONS

In this study, CBMC and MD simulations were carried out to investigate the volume swelling and the viscosity reduction of the n-alkane/ CO_2 systems. Results from the CBMC simulations indicate that pressure, temperature, and oil composition are the main factors impacting the CO_2 solubility, density, and swelling factor of the n-alkane/ CO_2 system. Both the CO_2 solubility and the swelling factor of the n-alkane/ CO_2 system increase with increasing pressure and decreasing temperature. The CO_2 solubility and swelling effect are more pronounced in light oil. The pressure and the temperature have a negligible effect on the density of pure n-alkanes, while the density of CO_2 -saturated n-alkanes decreases dramatically with the increasing pressure and the decreasing temperature. The interaction energy between n-alkanes and CO_2 can reasonably explain the swelling process.

The MD simulation results show that the viscosity of the n-alkane/ CO_2 system is approximately in an inversely proportional relationship with the mole fraction of dissolved CO_2 . The average viscosity reduction rate is about 45% when the CO_2 mole fraction is 60%. However, the viscosity of the mixture is still much higher than the CO_2 viscosity. In order to enhance the oil recovery with CO_2 injection, more research should focus on controlling the CO_2 mobility and improving the sweeping efficiency.

Molecular simulation studies provide better insight into the interactions between oil components and CO_2 at the molecular level. The application of molecular simulation methods can play an important role in interpreting experimental results and providing guidance for practical oil recovery processes in the Bakken Formation.

AUTHOR INFORMATION

Corresponding Authors

*E-mail: hui.pu@und.edu. Tel.: (+1) 701-777-6861.

*E-mail: julia.zhao@und.edu. Tel.: (+1) 701-777-3610.

ORCID ®

Hui Pu: 0000-0003-3074-3705

Julia Xiaojun Zhao: 0000-0002-9603-666X

Notes

The authors declare no competing financial interest.

ACKNOWLEDGMENTS

The authors thank the North Dakota Industrial Commission, Oil and Gas Research Program (G-041-081) and National Science Foundation (NSF1709160) for the financial support.

REFERENCES

- (1) Suebsiri, J.; Wilson, M.; Tontiwachwuthikul, P. Life-Cycle Analysis of CO₂ EOR on EOR and Geological Storage through Economic Optimization and Sensitivity Analysis Using the Weyburn Unit As a Case Study. *Ind. Eng. Chem. Res.* **2006**, *45*, 2483–2488.
- (2) Manrique, E. J.; Muci, V. E.; Gurfinkel, M. E. EOR Field Experiences in Carbonate Reservoirs in the United States. *SPE Reserv. Eval. Eng.* **2007**, *10*, 667–686.
- (3) Kuuskraa, V. A.; Godec, M. L.; Dipietro, P. CO₂Utilization from "Next Generation" CO₂Enhanced Oil Recovery Technology. *Energy Procedia* **2013**, *37*, 6854–6866.
- (4) Alvarado, V.; Manrique, E. Enhanced Oil Recovery: an Updated Review. *Energies* **2010**, *3*, 1529–1575.
- (5) Sorensen, J. A.; Braunberger, J. R.; Liu, G.; Smith, S. A.; Klenner, R. C. L.; Steadman, E. N.; Harju, J. A. CO₂Storage and Utilization in Tight Hydrocarbon-Bearing Formations: a Case Study of the Bakken Formation in the Williston Basin. *Energy Procedia* **2014**, *63*, 7852−7860.
- (6) LeFever, J.; Helms, L. Bakken Formation Reserve Estimates. *Executive Summary*; North Dakota Geological Survey: 2006.
- (7) Clark, A. J. Determination of Recovery Factor in the Bakken Formation, Mountrail County, ND. Society of Petroleum Engineers. 2009, 1.
- (8) Yu, W.; Lashgari, H.; Sepehrnoori, K. Simulation Study of CO₂Huff-n-Puff Process in Bakken Tight Oil Reservoirs. *Society of Petroleum Engineers.* **2014**, 1.
- (9) Orr, F. M.; Heller, J. P.; Taber, J. Carbon Dioxide Flooding for Enhanced Oil Recovery: Promise and Problems. *J. Am. Oil Chem. Soc.* **1982**, *59*, 810A–817A.
- (10) Seyyedsar, S. M.; Farzaneh, S. A.; Sohrabi, M. Investigation of Low-Density CO₂ Injection for Enhanced Oil Recovery. *Ind. Eng. Chem. Res.* **2017**, *56* (18), 5443–5454.
- (11) Yang, Z.; Li, M.; Peng, B.; Lin, M.; Dong, Z. Dispersion Property of CO_2 in Oil Part 1: Volume Expansion of CO_2 + Alkane at Near Criticaland Supercritical Condition of CO_2 . *J. Chem. Eng. Data* **2012**, *57*, 882–889.
- (12) Zheng, S.; Li, H.; Sun, H.; Yang, D. Determination of Diffusion Coefficient for Solvent-CO₂Mixtures in Heavy Oil with Consideration of Swelling Effect. *Ind. Eng. Chem. Res.* **2016**, *55*, 1533–1549.
- (13) Mosavat, N.; Abedini, A.; Torabi, F. Phase Behavior of CO₂-Brine and CO₂-Oil Systems for CO₂Storage and Enhanced Oil Recovery: Experimental Studies. *Energy Procedia* **2014**, *63*, 5631–5645.
- (14) Han, H.; Yuan, S.; Li, S.; Liu, X.; Chen, X. Dissolving Capacity and Volume Expansion of Carbon Dioxide in Chain N-Alkanes. *Pet. Explor. Dev.* **2015**, 42 (1), 97–103.
- (15) Dong, X.; Shi, Y.; Yang, D. Quantification of Mutual Mass Transfer of CO_2/N_2 -Light Oil Systems by Dynamic Volume Analysis. *Ind. Eng. Chem. Res.* **2018**, *57*, 16495–16507.
- (16) Simon, R.; Graue, D. Generalized Correlations for Predicting Solubility, Swelling, and Viscosity Behavior of CO₂-Crude Oil Systems. *JPT, J. Pet. Technol.* **1965**, *17*, 102–106.
- (17) Mulliken, C. A.; Sandler, S. I. The Prediction of CO₂ Solubility and Swelling Factors for Enhanced Oil Recovery. *Ind. Eng. Chem. Process Des. Dev.* **1980**, 19 (4), 709–711.

- (18) Chung, F. T. H.; Jones, R. A.; Nguyen, H. T. Measurement and Correlations of the Physical Properties of CO₂/Heavy-Crude-Oil Mixtures. SPE Reservoir Eng. 1988, 3, 822–828.
- (19) Macías-Salinas, R.; Chavez-Velasco, J. A.; Aquino-Olivos, M. A.; Mendoza de la Cruz, J. L.; Sanchez-Ochoa, J. C. Accurate Modeling of CO₂ Solubility in Ionic Liquids Using a Cubic EoS. *Ind. Eng. Chem. Res.* **2013**, *52*, 7593–7601.
- (20) Liu, H.; Dai, S.; Jiang, D. Molecular Dynamics Simulation of Anion Effect on Solubility, Diffusivity, and Permeability of Carbon Dioxide in Ionic Liquids. *Ind. Eng. Chem. Res.* **2014**, *53*, 10485–10490.
- (21) Vorholz, J.; Harismiadis, V. I.; Panagiotopoulos, A. Z.; Rumpf, B.; Maurer, G. Molecular Simulation of the Solubility of Carbon Dioxide in Aqueous Solutions of Sodium Chloride. *Fluid Phase Equilib.* **2004**, 226, 237–250.
- (22) Urukova, I.; Perez-Salado Kamps, A.; Maurer, G. Solubility of CO₂ in (Water + Acetone): Correlation of Experimental Data and Predictions from Molecular Simulation. *Ind. Eng. Chem. Res.* **2009**, *48*, 4553–4564.
- (23) Zhang, J.; Pan, Z.; Liu, K.; Burke, N. Molecular Simulation of CO₂Solubility and Its Effect on Octane Swelling. *Energy Fuels* **2013**, 27, 2741–2747.
- (24) Liu, B.; Shi, J.; Sun, B.; Shen, Y.; Zhang, J.; Chen, X.; Wang, M. Molecular dynamics Simulation on Volume Swelling of CO₂-Alkane System. *Fuel* **2015**, *143*, 194–201.
- (25) Moultos, O. A.; Tsimpanogiannis, I. N.; Panagiotopoulos, A. Z.; Trusler, J. P. M.; Economou, I. G. Atomistic Molecular Dynamics Simulations of Carbon Dioxide Diffusivity in n-Hexane, n-Decane, nHexadecane, Cyclohexane, and Squalane. *J. Phys. Chem. B* **2016**, *120*, 12890–12900.
- (26) Sorensen, J. A.; Hawthorne, S. B.; Jin, L.; Kurz, B. A.; Smith, S. A.; Azenkeng, A. Laboratory Characterization and Modeling to Examine CO₂Storage and Enhanced Oil Recovery in An Unconventional Tight Oil Formation. *The 13th International Conference on Greenhouse Gas Control Technologies.* **2017**, 5460.
- (27) Hawthorne, S. B.; Miller, D. J.; Grabanski, C. B.; Sorensen, J. A.; Pekot, L. J.; Kurz, B. A.; Gorecki, C. D.; Steadman, E. N.; Harju, J. A.; Melzer, S. Measured Crude Oil MMPs with Pure and Mixed CO₂, Methane, and Ethane, and Their Relevance to Enhanced Oil Recovery from Middle Bakken and Bakken Shales. *Society of Petroleum Engineers*. 2017. 1.
- (28) Kurtoglu, B. Integrated Reservoir Characterization and Modeling in Support of Enhanced Oil Recovery for Bakken. Ph.D. Dissertation, Colorado School of Mines, Golden, CO, 2013.
- (29) Siepmann, J. I.; Frenkel, D. Configurational Bias Monte Carlo: A New Sampling Scheme for Flexible Chains. *Mol. Phys.* **1992**, *75* (1), 59–70.
- (30) Frenkel, D.; Mooij, G. C. A. M.; Smit, B. Novel Scheme to Study Structural and Thermal Properties of Continuously Deformable Molecules. *J. Phys.: Condens. Matter* **1992**, *4* (12), 3053–3076.
- (31) Martin, M. G.; Siepmann, J. I. Transferable Potentials for Phase Equilibria. 1. United-Atom Description of N-Alkanes. *J. Phys. Chem. B* **1998**, *102*, 2569–2577.
- (32) Martin, M. G.; Siepmann, J. I. Novel Configurational-Bias Monte Carlo Method for Branched Molecules. Transferable Potentials for Phase Equilibria: 2. United-Atom Description of Branched Alkanes. *J. Phys. Chem. B* **1999**, *103*, 4508–4517.
- (33) Siu, S. W. I.; Pluhackova, K.; Bockmann, R. A. Optimization of the OPLS-AA Force Field for Long Hydrocarbons. *J. Chem. Theory Comput.* **2012**, 8 (4), 1459–1470.
- (34) Ewen, J. P.; Gattinoni, C.; Thakkar, F. M.; Morgan, N.; Spikes, H. A.; Dini, D. A Comparison of Classical Force-Fields for Molecular Dynamics Simulations of Lubricants. *Materials* **2016**, *9*, 651–668.
- (35) Potoff, J. J.; Siepmann, J. I. Vapor-Liquid Equilibria of Mixtures Containing Alkanes, Carbon Dioxide, and Nitrogen. *AIChE J.* **2001**, 47, 1676–1682.
- (36) Dubbeldam, D.; Calero, S.; Vlugt, T. J. H.; Krishna, R.; Maesen, T. L. M.; Smit, B. J. United Atom Force Field for Alkanes in Nanoporous Materials. *J. Phys. Chem. B* **2004**, *108*, 12301–12313.

- (37) Green, M. S. Markoff Random Processes and the Statistical Mechanics of Time-Dependent Phenomena. II. Irreversible Processes in Fluids. *J. Chem. Phys.* **1954**, *22*, 398–413.
- (38) Kubo, R. Statistical-Mechanical Theory of Irreversible Processes. I. General Theory and Simple Applications to Magnetic and Conduction Problems. J. Phys. Soc. Jpn. 1957, 12, 570–586.
- (39) Hockney, R. W.; Eastwood, J. W Computer Simulation Using Particles; CRC Press: NY, 1989.
- (40) Nose, S. A Unified Formulation of the Constant Temperature Molecular Dynamics Methods. *J. Chem. Phys.* **1984**, *81*, 511–519.
- (41) Hoover, W. Q.; Ladd, A. J. C.; Moran, B. High-Strain-Rate Plastic Flow Studied via Nonequilibrium Molecular Dynamics. *Phys. Rev. Lett.* **1982**, *48*, 1818.
- (42) Parrinello, M.; Rahman, A. Polymorphic Transitions in Single Crystals: A New Molecular Dynamics Method. *J. Appl. Phys.* **1981**, *52*, 7182–7190.
- (43) Ryckaert, J. P.; Ciccotti, G.; Berendsen, H. J. C. Numerical-Integration of Cartesian Equations of Motion of A System with Constraints—Molecular-Dynamics of N-Alkanes. *J. Comput. Phys.* 1977, 23, 327–341.
- (44) Dubbeldam, D.; Calero, S.; Ellis, D. E.; Snurr, R. Q. RASPA: Molecular Simulation Software for Adsorption and Diffusion in Flexible Nanoporous Materials. *Mol. Simul.* **2016**, *42*, 81–101.
- (45) Plimpton, S. Fast Parallel Algorithms for Short-Range Molecular Dynamics. *J. Comput. Phys.* **1995**, *117*, 1–19.
- (46) Humphrey, W.; Dalke, A.; Schulten, K. VMD: Visual Molecular Dynamics. J. Mol. Graphics 1996, 14 (1), 33–38.
- (47) Lemmon, E. W.; McLinden, M. O.; Friend, D. G.; Linstrom, P. J.; Mallard, W. G NIST Chemistry Webbook, 2014.